Nuclear Engineering and Technology 55 (2023) 215–221

Contents lists available at ScienceDirect

Nuclear Engineering and Technology

journal homepage: www.elsevier.com/locate/net

Original Article

Investigating the effects of a range shifter on skin dose in proton therapy

Ming Wang [a, b, *], Lei Zhang [a], Jinxing Zheng [b], Guodong Li [a], Wei Dai [a], Lang Dong [a]

[a] Chengdu University of Technology, Chengdu, 610059, China
[b] Institute of Plasma Physics, Chinese Academy of Sciences, Hefei, 230031, China

ARTICLE INFO

Article history:
Received 29 June 2022
Received in revised form
28 August 2022
Accepted 15 September 2022
Available online 20 September 2022

Keywords:
Proton therapy facility
Range shifter
Skin dose
Airgap

ABSTRACT

Proton treatment may deliver a larger dose to a patient's skin than traditional photon therapy, especially when a range shifter (RS) is inserted in the beam path. This study investigated the effects of an RS on skin dose while considering RS with different thicknesses, airgaps and materials. First, the physical model of the scanning nozzle with RS was established in the TOol for PArticle Simulation (TOPAS) code, and the effects of the RS on the skin dose were studied. Second, the variations in the skin dose and isocenter beam size were examined by reducing the air gap. Finally, the effects of different RS materials, such as polymethylmethacrylate (PMMA), Lexan, polyethylene and polystyrene, on the skin dose were analysed. The results demonstrated that the current RS design had a negligible effect on the skin dose, whereas the RS significantly impacted the isocenter beam size. The skin dose was increased considerably when the RS was placed close to the phantom. Moreover, the magnitude of the increase was related to the thickness of the inserted RS. Meanwhile, the results also revealed that the secondary proton primarily contributed to the increased skin dose.

1. Introduction

Because of its excellent dose distribution, proton treatment can significantly reduce irradiation damage to additional tissues and has become a growing trend in cancer radiation therapy [1]. However, energy is deposited proximal to the tumour in the entrance channel during tumour irradiation. This action may result in undesirable side effects such as skin irritation [2,3]. Besides, higher skin toxicity in proton than photon irradiation could be related to a higher skin dose [4].

The skin is placed inside the proton field dose gradient caused by the primary proton linear energy transfer and the secondary particles that develop during proton treatment. The deposited dose may damage the skin [5,6]. The build-up dose mainly comprises two parts: one from a short-range electron build-up downstream of the air-patient contact and the other from a nuclear build-up [7]. Short-range electrons, in particular, significantly affect the skin dose because they deposit their energy mostly locally. A range shifter (RS) is a specific device in the nozzle that regulates energy to treat shallow tumours [8,9], while the energy-modulating process generates a large number of secondary particles [10]. Air, which serves as the medium between the RS and the skin, has low stopping power, which greatly increases the chances of these particles entering the human body. Therefore, it is essential to comprehensively examine the effects of RS on the skin dose, especially when the RS is placed closer to the patient.

Kelleter et al. used the Monte Carlo method to analyse the magnitude of the electron and proton build-up for different energies, as well as the impact of the airgap on the magnitude of both effects [11]. Kern et al. investigated the effects of the airgap, RS and delivery technique on the skin dose [12]. Previous research have studied the impact of the distance between the nozzle and the phantom on the skin dose while examining the skin dose variation caused by an RS. In fact, the proton centres generally provide RS with different thicknesses to fulfil the requirements of clinical energy modulation for different types of tumours. The RS's thickness will be coupled with parameters such as airgap and materials to affect the changes in the skin dose and isocenter beam size. Therefore, a detailed assessment of skin dose changes at different RS thicknesses is vital. This result will provide a reference for future dose optimisation and proton therapy device design.

The purpose of this research is to investigate the effects of an RS

* Corresponding author. Chengdu University of Technology, Chengdu, 610059, China.
E-mail address: wangming1@cdut.edu.cn (M. Wang).

https://doi.org/10.1016/j.net.2022.09.016

on the skin dose. First, the physical model of the scanning nozzle with RS was established in the Monte Carlo code TOol for PArticle Simulation (TOPAS) code [13], and the effects of the RS on the skin dose were investigated. Second, the variation in the skin dose was examined while reducing the impact of the RS on the isocenter's beam size. Finally, the effects of RS with different materials on skin dose were also explored.

2. Materials and methods

2.1. SC200 PBS nozzle with a range shifter

The SC200 superconducting cyclotron for proton therapy is under development in Hefei. It is designed to accelerate protons to 200 MeV with a maximum beam current of 1 μA [14]. There are two treatment rooms in SC200: one is a gantry treatment room and the other is a fixed-beam treatment room. Both treatment rooms use an active scanning technology as the beam transport method to take full advantage of the physical benefits of protons [14]. An RS is added at the exit position of the scanning nozzle to realise the irradiation treatment of superficial tumours. Fig. 1 depicts the geometric relationship between the nozzle and the RS.

For the current RS design of the SC200 proton therapy device, RS is fixed at the scanning nozzle install plate. The distance between the RS and the isocenter is 70.0 cm (airgap = 79.0 cm). The material of RS comprises polymethylmethacrylate (PMMA). The RS plates are designed with four water equivalent thicknesses, namely 5.2 mm, 10.4 mm, 20.8 mm and 41.2 mm, to meet the needs of fine energy regulation (the corresponding physical thicknesses of the PMMA plates are 4.5 mm, 9.0 mm, 18.0 mm and 36.0 mm). The RS4.5, RS9, RS18 and RS36 will be used instead of the RS with thicknesses of 4.5 mm, 9.0 mm, 18 mm and 36 mm to easily distinguish the RS of the four thicknesses.

2.2. The skin dose calculation method

The International Commission on Radiological Protection recommends assessing the skin dose at a depth of 0.07 mm (basal layer), whereas the dermal layer may be examined at 1.0 mm [15–17]. The dose to the basal layer (0.07 mm) is often used interchangeably with the skin dose for conventional photons or proton therapy [10,11,17–20]. Therefore, the dose deposited at 70 μm was also used to represent the skin dose in this paper.

In this study, one pencil beam scanning nozzle, including the RS, was established in the TOPAS code. Meanwhile, this study was conducted by referring to the previous method of proton dose analysis, that is, normalising the dose obtained at 70 μm with the dose at 3 cm [6,7]. This Monte Carlo simulation used the default physical models of TOPAS, which have been investigated in detail by Paganetti and Zacharatou [21]. The number of particles simulated in each scenario was 5×10^6.

3. Results

3.1. Effect of the range shifter on the skin dose

Fig. 2 illustrates the skin doses standardised to a depth of 3 cm for quasimonoenergetic energies from 80 to 200 MeV in steps of 20 MeV. The effect of the RS with different thicknesses on the skin dose was also investigated. Furthermore, the skin dose value without the RS (RS0) is added to the figure for reference to demonstrate the effect of the RS on the skin dose more deftly. The distance between the RS and the isocenter is 70.0 cm for this stimulation.

Fig. 2 shows that, in the absence of RS, the skin dose increases with increasing incident energy. However, increasing skin dose gradually declines with more incident energy. The skin dose was reduced when an RS was inserted in the beam path. Moreover, the magnitude of the reduction in skin dose was proportional to the thickness of the inserted RS.

Table 1 presents the skin dose ratios of a proton beam produced by the beam energy modulation using RS4.5, RS9, RS18 and RS36 compared with a monoenergetic proton beam in the same range but without an RS. In this table, the incident energy represents the proton beam energy before entering the RS, and Equ_E represents the average proton energy modulated by the RS. The table shows that the skin dose ratio for all cases is almost equal to 1 when the

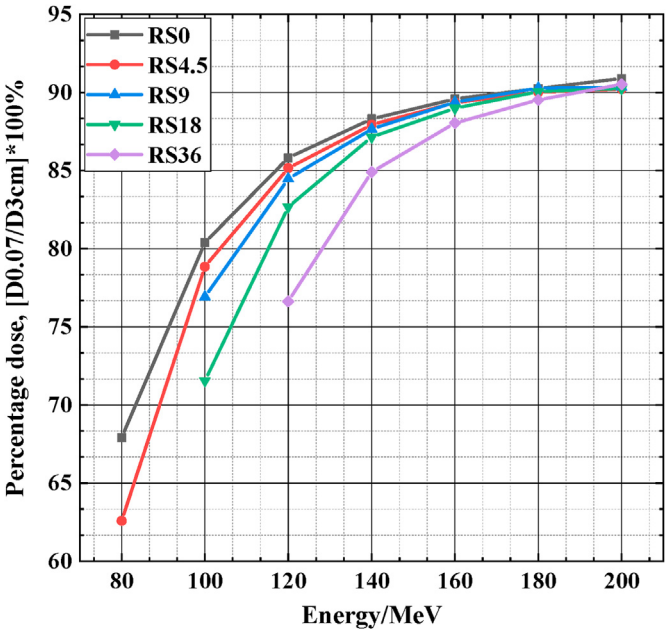

Fig. 2. Variation of skin dose under different range shifter thickness modulation.

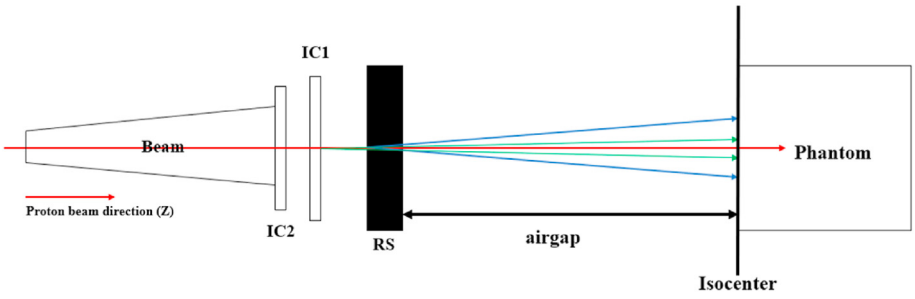

Fig. 1. Schematic diagram of the position of the RS and the pencil beam scanning nozzle.

Table 1
The skin dose ratios of a proton beam with an RS than a monoenergetic proton beam with the same range but without an RS.

Incident energy MeV	RS4.5		RS9		RS18		RS36	
	Equ_E	Ratio	Equ_E	Ratio	Equ_E	Ratio	Equ_E	Ratio
200	196.90	0.99	194.50	1.00	189.80	1.00	180.10	1.00
180	176.60	1.00	174.10	1.00	169.10	1.00	158.60	1.00
160	156.40	1.00	153.60	1.00	148.10	1.00	136.50	1.00
140	136.00	1.00	133.00	1.00	126.80	1.00	113.80	1.00
120	115.50	1.00	112.10	1.00	105.10	1.00	89.90	1.00
100	94.90	1.00	90.90	1.00	82.60	1.00	–	–
80	73.80	1.01	–	–	–	–	–	–

incident energy varies in the range of 80–200 MeV. This result indicates that the effects of the secondary particles generated during beam modulation on the skin dose are negligible for the current RS design (air gap = 70 cm).

3.2. Effect of the range shifter on the isocenter beam size

The outcomes in Fig. 2 demonstrate that the current RS design does not affect the skin dose. However, the effect of the RS on the isocenter beam size must also be considered in the design phase. Especially for the scanning dose delivery technology, the size of the isocenter beam spot is closely related to the uniformity of the final target dose distribution [8,10].

Fig. 3(A) shows the effect on the isocenter beam size after considering the RS. The results evinced that the RS significantly affects the beam spot size, especially when the inserted RS is thicker and the beam energy is lower.

Fig. 3(B) shows the variations in the beam size when the airgaps were 70 cm, 60 cm, 50 cm, 40 cm, 30 cm, 20 cm, 10 cm and 5 cm. Only proton beams with beam energies of 70 MeV and 100 MeV were used in Fig. 3(B) because the beam scattering is considered more sensitive to low-energy protons. Fig. 3(B) reveals that the beam size at the isocenter is significantly improved with the reduced airgap. Meanwhile, these results also demonstrate that the RS exerted little effect on the isocenter beam size when the airgap was about 5 cm. Actually, the RS could not be placed closer to the patient; therefore, these results provide a reference for the subsequent RS optimisation.

3.3. Effect of distance adjustment between the range shifter and isocenter on the skin dose

Section 3.2 shows that the influence of the RS on the isocenter beam size becomes very minimal when the airgaps are about 5 cm. However, the secondary particles generated during the energy-modulated process have a greater chance of entering the body when the RS approaches the phantom's surface.

Fig. 4 presents the relationship between skin dose and airgap at four thicknesses: RS4.5, RS9, RS18 and RS36. In addition, the reference skin dose value is added in each figure to clearly demonstrate the effects of secondary particles on the skin dose with the change in the airgaps. The incident energy corresponding to the reference skin dose is Equ_E, and the meaning of Equ_E was explained in Section 3.1.

Fig. 4 shows that the effect of secondary particles generated during energy modulation on the skin dose is manifested for the RS of the same thickness upon reducing the airgap. Especially when the RS was very close to the phantom surface, a significant increase was observed in the skin dose. Meanwhile, the results also revealed that the increased value in the skin dose is proportional to the thickness of the inserted RS. Corresponding to the RS 4.5, RS9, RS 18 and 36 thicknesses of the RS, the maximum increase in the skin dose caused by them was divided into 2%, 3%, 4% and 5%, respectively. Combining the results of Figs. 3 and 4 showed that the position of the RS can be kept at a distance from the skin to reduce the influence of the RS on the skin dose and the beam spot during radiotherapy. When this distance was around 5 cm, the RS had little effect on the beam size and the increase of the skin dose was not also evident.

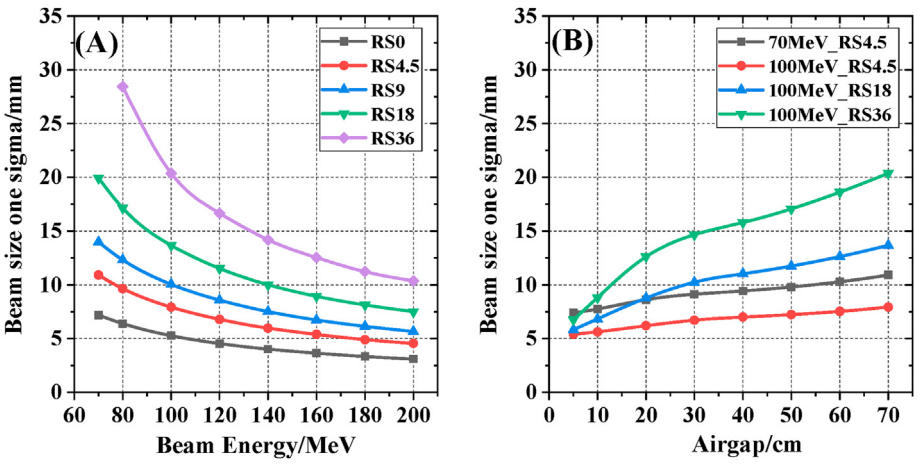

Fig. 3. Beam size after modulation at the isocenter
(A: Beam size in the *x*-direction; B: Beam size changes in the *y*-direction).

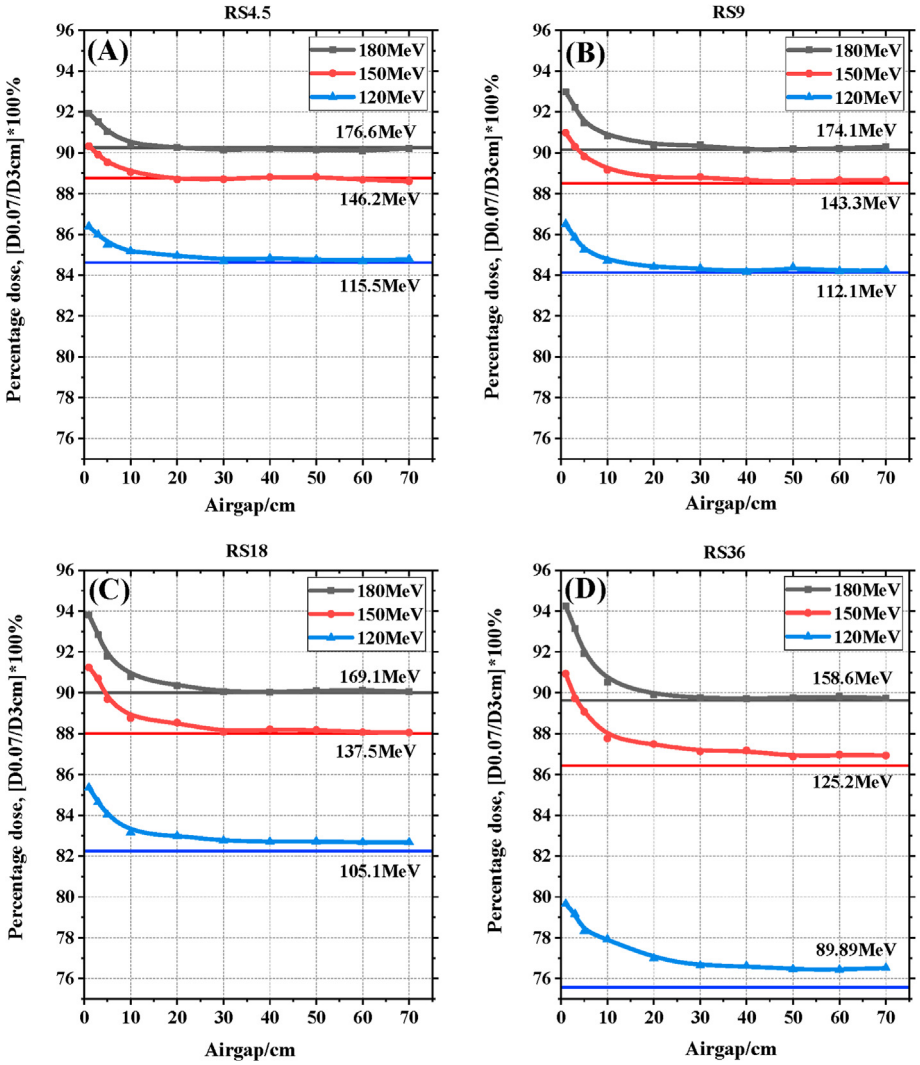

Fig. 4. The skin dose variation with different range shifter thicknesses (A: The thickness of the range shifter is 4.5 mm; B: The thickness of the range shifter is 9 mm; C: The thickness of the range shifter is 18 mm; D: The thickness of range shifter is 36 mm).

Fig. 5 displays the particle contribution to the skin dose and the related particle energy spectrum. Fig. 5(A) shows the particle flux on the phantom's surface when the RS36 and airgap are 10 cm. Fig. 5(A) also reveals that the initial proton flux accounts for the highest proportion, about 95.6%. The particles with the highest proportion of secondary particles are secondary protons, electrons, neutrons and photons.

Fig. 5(B) presents the relationship of the energy spectrum of the secondary proton incident on the surface of the phantom with the change in the airgaps. This figure considers the secondary proton energy spectrum distributions of proton beams at 120 MeV and 180 MeV of energy with airgaps of 5 cm, 10 cm and 20 cm. The figure shows that the number of particles incident on the surface of the phantom increases significantly for the same incident energy with the increase in the airgap. The number of incident secondary protons decreases when the airgap increases because they do not enter the phantom space because of the large scattering angle during the reaction.

Fig. 5(C) considers the electrons' energy spectrum distributions of proton beams at 120 MeV and 180 MeV of energy with air gaps of 1 cm, 5 cm, 10 cm and 20 cm. This figure shows that the energy of the secondary electrons is mainly concentrated in the range of 0.1 MeV–0.5 MeV. The counted electrons increase with the decrease in the air gap.

Fig. 5(D) shows the electron energy spectrum distribution at the outlet of the RS and the inlet of the phantom. This figure shows the energy of the particles generated at the outlet of the RS is higher than that obtained by the statistics at the phantom's inlet. The results demonstrated that the air between the RS and the phantom also exerted a particular blocking effect on the electron. In this figure, 120 MeV_RS represents the energy distribution of the beam with an incident energy of 120 MeV at the outlet of the RS, and the 120 MeV_Phantom represents the energy distribution of the beam with an incident energy of 120 MeV at the phantom's inlet.

Fig. 6(A) shows the contribution of different particles to the skin dose with different air gaps. The skin dose is mainly contributed by the initial proton (pri_proton). The proportion of the secondary particle dose particularly comes from secondary protons (sec_proton) and electrons (electrons). In Fig. 6, the symbol of others represents the dose deposited from all the particles, excluding primary and secondary proton and electron. Fig. 6(B) shows the contribution of secondary particles to the skin dose with different air gaps. This figure shows that when the air gap gets smaller, the proportion of the dose contributed by the secondary protons

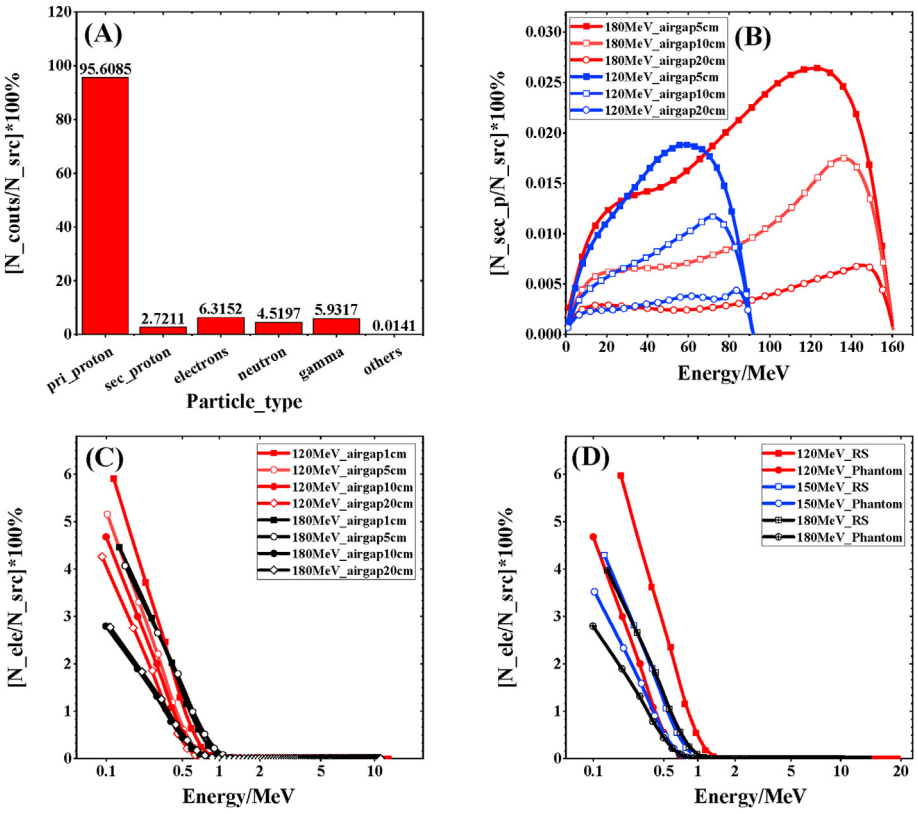

Fig. 5. The energy spectrum distribution of the secondary particles with different airgaps (A: Percentage of the particle flux at the phantom inlet; B: Secondary proton energy spectrum distribution under different air gaps at the phantom's inlet; C: Secondary electron energy spectrum distribution under varying air gaps at the inlet of the phantom; D: Secondary electron energy spectrum distribution at the outlet of the range shifter and the inlet of the phantom. In this figure, N_counts represent the particle counts; N_src represents the primary proton number; N_sec_p represents the secondary proton counts; and N_ele represents the electron counts.).

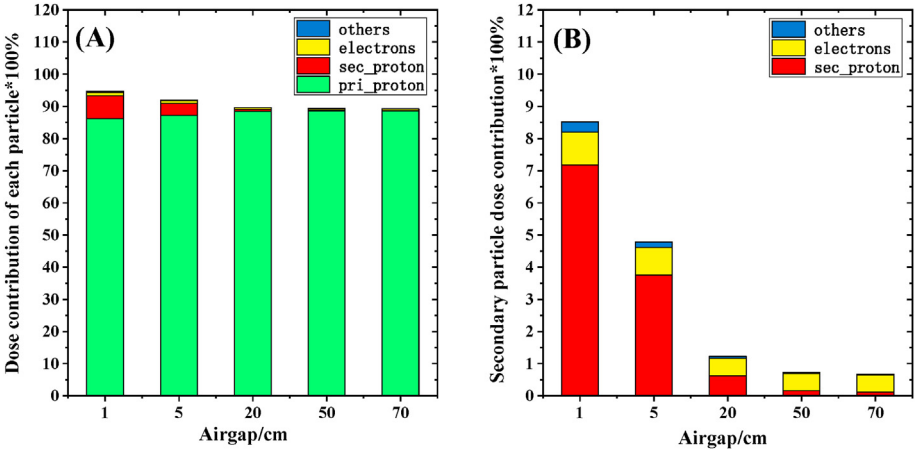

Fig. 6. Contribution of different particles on the skin dose with different airgaps (A: the skin dose ratio contributed by all particles; B: the skin dose ratio contributed by secondary particles).

increases; however, the dose contributed by the electrons does not change significantly. This finding indicates that when the RS and the isocenter distance are reduced, the increase in the skin dose is attributed to the deposition of the secondary particle dose. Moreover, secondary protons primarily contributed to the rise in the skin dose.

3.4. Effect of range shifter materials on the skin dose

The RS materials currently used in proton devices are PMMA, polyethylene, Lexan and Polystyrene. The RS material selected by the IBA Proton Device Commercial Company is Lexan. The Swiss PSI Proton Center has selected polyethylene. In contrast, MGH of the

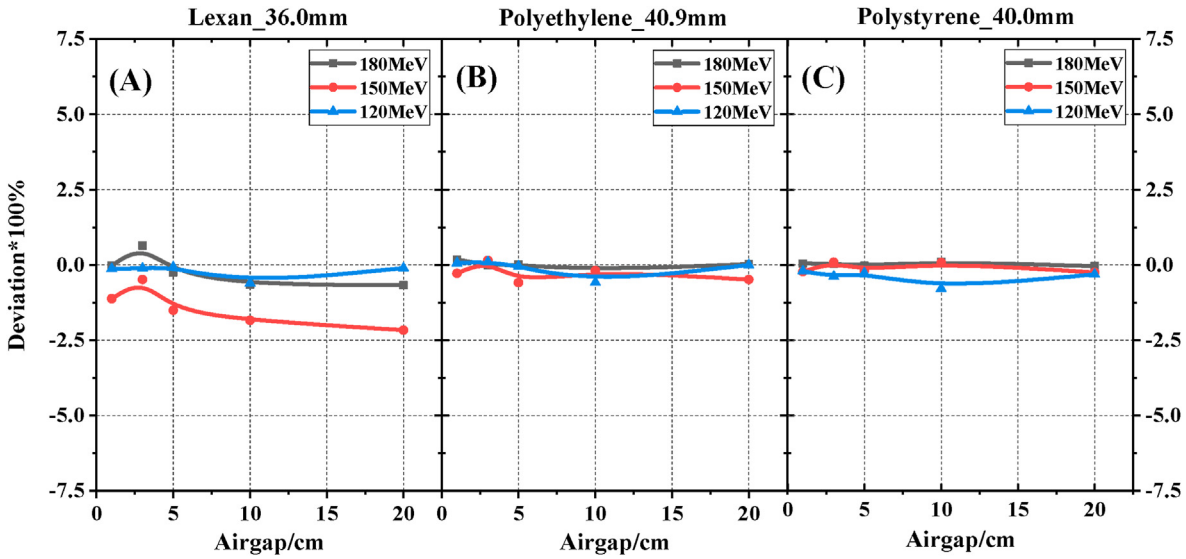

Fig. 7. Presents a comparison of the effects of several range shifter materials on the surface skin dose.

Massachusetts General Hospital has selected PMMA. Several researchers have also investigated the effects of different RS materials on the isocenter beam size [8–10]. However, to the best of the authors' knowledge, an evaluation of the skin dose induced by different RS materials has not yet been discovered.

Fig. 7 shows the skin dose ratios produced using Lexan, polyethylene and polystyrene as the RS material versus PMMA as the RS material. Considering the water equivalent thickness of different materials and achieving the same range modulation (41.2 mm), Lexan, polyethylene and polystyrene have set physical thicknesses of 36 mm, 40.9 mm and 40 mm, respectively. Fig. 7 shows that the skin doses caused by the above four materials were basically the same when the RS was inserted in the beam path, with no significant difference.

4. Conclusion

Proton therapy (due to the physical of the Bragg curve) offers distinct dose advantages over other conventional photon or electron techniques. Therefore, it has paved the development direction of modern radiation. However, some studies showed higher skin toxicity in protons than photon irradiation, which could be attributed to a higher skin dose. This paper evaluated the effects of the RS on skin dose, as well as the relationship between skin dose variation and the thickness of RS, air gaps and materials. The Monte Carlo code TOPAS was used in this research.

The effect of RS on the skin dose is negligible for the current nozzle design (air gap = 70 cm). However, the isocenter beam size expansion caused by the RS is very evident. The enlarged isocenter beam spot problem has been significantly improved with the decrease in the air gap. When the air gap is less than 20 cm, secondary particles generated during the energy-modulated process have more chance to enter the phantom. Notably, the skin dose presented a marked increase. Meanwhile, the increase in the superficial skin dose was proportional to the thickness of the inserted range shifter. Corresponding to the thicknesses of RS 4.5, RS9, RS 18 and RS 36, the maximum increase in the skin dose caused by them was divided into 2%, 3%, 4% and 5%, respectively. Secondary protons primarily contributed to the increase of the skin dose.

The effect of four common materials, namely Lexan, polyethylene, polystyrene and PMMA, on the skin dose was also examined. The results revealed that these materials had essentially the same effect on the skin dose. Combined with clinical practice, the research results also showed that the isocenter beam size and the skin dose increase are within a small range when the air gap is kept at about 5 cm. These analysis results will serve as technical references for the further optimisation of the RS. Moreover, this study did not assess the relative biological effects of distance caused by these secondary particles or the variation between LETs. The following phase involves analysing and researching the local micro- or nano-dose using precise treatment planning data.

Declaration of competing interest

The authors declare that they have no known competing financial interests or personal relationships that could have appeared to influence the work reported in this paper.

Acknowledgement

The authors wish to thank all of the members of the SC200 design team. The National Natural Science Foundation of China (No. 12105030), and the Scientific Research Foundation of the Education Department of Sichuan Province, China, have all contributed to this research (No.2022NSFSC1185).

Appendix A. Supplementary data The attachment is a proof of the language modification of the article, which is not closely related to the research content of the article. Could you please remove this attachment from the manuscript?

Supplementary data to this article can be found online at https://doi.org/10.1016/j.net.2022.09.016.

References

[1] H. Paganetti, T. Bortfeld, Springer, Berlin, Heidelberg, 2006, pp. 345–363. Proton therapy[M]//New technologies in radiation oncology.
[2] Y. Lee, K. Hwang, Skin thickness of Korean adults[J], Surgical and radiologic anatomy 24 (3) (2002) 183–189.
[3] ICRU Report No. 39, Determination of dose equivalents resulting from external radiation sources, International Commission on Radiation Units and Measurements (1985).
[4] J.J. Cuaron, C. Cheng, H. Joseph, et al., Dosimetric comparison of skin surface

dose in patients undergoing proton and photon radiation therapy for breast cancer[J], International Journal of Radiation Oncology, Biology, Physics 90 (1) (2014) S914.
[5] C.A. Carlsson, G.A. Carlsson, Proton dosimetry with 185 MeV protons[J], Health physics 33 (5) (1977) 481–484.
[6] A. Kern, C. Bäumer, K. Kröninger, et al., Determination of surface dose in pencil beam scanning proton therapy[J], Medical Physics 47 (5) (2020) 2277–2288.
[7] T. Pfuhl, F. Horst, C. Schuy, et al., Dose build-up effects induced by delta electrons and target fragments in proton Bragg curves—measurements and simulations[J], Physics in Medicine & Biology 63 (17) (2018), 175002.
[8] J. Shen, W. Liu, A. Anand, et al., Impact of range shifter material on proton pencil beam spot characteristics[J], Medical physics 42 (3) (2015) 1335–1340.
[9] R. PIDIKITI, B.C. PATEL, M.R. MAYNARD, et al., Commissioning of the world's First compact pencil-beam scanning proton therapy system[J], Journal of applied clinical medical physics 19 (1) (2018) 94–105.
[10] Y.G.H. YU, Y. HU, et al., Study on the influence of the range shifter material in a scanning nozzle for proton therapy based on Monte Carlo method[C], 10th Int. Partile Accelerator Conf.(IPAC'19) (19-24 May 2019) 4100–4102.
[11] L. Kelleter, B. Zhen-Hong Tham, R. Saakyan, et al., Simulation of dose buildup in proton pencil beams[J], Medical Physics 46 (8) (2019) 3734–3738.
[12] A. Kern, C. Bäumer, K. Kröninger, et al., Impact of air gap, range shifter, and delivery technique on skin dose in proton therapy[J], Medical Physics 48 (2) (2021) 831–840.
[13] J. Perl, J. Shin, J. Schümann, et al., TOPAS: an innovative proton Monte Carlo platform for research and clinical applications[J], Medical physics 39 (11) (2012) 6818–6837.
[14] M. Wang, J. Zheng, Y. Song, et al., Monte Carlo simulation using TOPAS for gas chamber design of PBS nozzle in superconducting proton therapy facility[J], Nuclear Technology 206 (5) (2020) 779–790.
[15] A.D. Wrixon, New recommendations from the international commission on radiological protection—a review[J], Physics in Medicine & Biology 53 (8) (2008) R41.
[16] M.J. Butson, J.N. Mathur, P.E. Metcalfe, Skin dose from radiotherapy X-ray beams: the influence of energy[J], Australasian radiology 41 (2) (1997) 148–150.
[17] B. Nilsson, B. Sorcini, Surface dose measurements in clinical photon beams[J], Acta Oncologica 28 (4) (1989) 537–542.
[18] P. Rapley, Surface dose measurement using TLD powder extrapolation[J], Medical Dosimetry 31 (3) (2006) 209–215.
[19] N. Dogan, G.P. Glasgow, Surface and build-up region dosimetry for obliquely incident intensity modulated radiotherapy 6 MV x rays[J], Medical Physics 30 (12) (2003) 3091–3096.
[20] S.F. Kry, S.A. Smith, R. Weathers, et al., Skin dose during radiotherapy: a summary and general estimation technique[J], Journal of applied clinical medical physics 13 (3) (2012) 20–34.
[21] C.Z. Jarlskog, H. Paganetti, Physics settings for using the Geant4 toolkit in proton therapy[J], IEEE Transactions on nuclear science 55 (3) (2008) 1018–1025.